LOW-VELOCITY IMPACT BEHAVIOR MODELLING OF BRAIDED TEXTILE COMPOSITES FOR SPORTS PROTECTION

Chen Wang[1,2,3], Anish Roy[1], Zhong Chen[2] and Vadim V. Silberschmidt[1*]

[1]Wolfson School of Mechanical and Manufacturing Engineering, Loughborough University, Leicestershire, LE11 3TU, U.K.
Email: C.Wang2@lboro.ac.uk, A.Roy3@lboro.ac.uk, V.Silberschmidt@lboro.ac.uk Web Page: http://www.lboro.ac.uk/departments/mechman/
[2] School of Materials Science and Engineering, Nanyang Technological University, 50 Nanyang Avenue, 639798, Singapore
Email: ASZChen@ntu.edu.sg, Web Page: http://www.mse.ntu.edu.sg/Pages/Home.aspx
[3]Institute for Sports Research, Nanyang Technological University, 50 Nanyang Avenue, 639798, Singapore
Web Page: http://www.isr.ntu.edu.sg/Pages/Home.aspx

Keywords: low-velocity impact, braided textile composite, dynamic damage, finite-element analysis

Abstract

Composites reinforced by braided textiles exhibit high structural stability and excellent damage tolerance. This makes braided composites very attractive for sports protection applications. A multi-scale computational approach is explored to predict low-velocity impact performance of braided textile composites. The computational model was supported by experimental verifications. A drop-weight test was carried out with a spike-shape impactor considering real sports impact collision scenarios. Impact energy levels ranged from 3 J to 9 J. The load- and energy-time curves were obtained both experimentally and numerically. Damage morphology was characterized employing X-ray micro computed-tomography scans. A predicted peak force and total strain energy were found to agree with experimental study. The main damage mechanisms of braided composites under low-velocity impact were delamination and matrix failure. The presented modelling capability will allow for design of braided composite structures for various dynamic loading scenarios.

1. Introduction

Textile-fabric-reinforced composites have received considerable attentions in recent years primarily due to high production volumes of textile preforms. Amongst various types of textiles, braided preforms provide high versatility in terms of fibre orientation and available preform cross-sections, which can then be made into near-net-shape of the final product [1-2]. The composites reinforced with braided textiles exhibit high structural stability and excellent damage tolerance thanks to the yarn interlacing. This makes braided composites very attractive for sports protection, e.g. body armour for hockey and shin guards for football players [3]. Therefore, studies of braided composites under impact loads become important.

For decades, extensive experiments were conducted to investigate impact behaviour of composites [4-6]. However, experiments can be time consuming and expensive. Additionally, damage under low-velocity impact conditions is difficult to detect experimentally. Therefore, there are strong needs to develop finite-element (FE) simulations tools capable of predicting dynamic behaviour of composites, considering multiple damage mechanisms [7]. Moura [8] proposed a double failure criterion based on a combination of classic failure theories such as Tsai-Wu, Hashin, *etc.* [9-10]. Hou et al. [5] implemented

Excerpt from ISBN 978-3-00-053387-7

an improved failure criterion for intra-ply damage modes and an empirical delamination model. Once damage was initiated, stiffness was reduced.

Composite damage models based on continuum damage mechanics (CDM) were increasingly investigated by many researchers, with energy dissipation associated with each failure mode (matrix cracking in tension and compression, fibre failure in tension and compression, and shear failure) independent of mesh refinement, element topology and fracture direction [9-14]. In recent simulation-based studies, cohesive elements were widely used to deal with delamination, regarded as the most important damage mode for composites exposed to low-velocity impacts. Long et al. [15] predicted delamination in composite laminates using a bilinear cohesive zone model. Qiu et al. [16] developed a surface-based cohesive interaction for prediction of initiation and propagation of delamination during impact. In general, a large number of factors affect the impact behaviour of composites, making its numerical modelling a challenge [18]. As a result, a universal numerical approach is missing.

This work aims at investigating a response of a braided composite to low-velocity impacts both experimentally and with FE simulations. Here, a crucial part of an ongoing work on multi-scale modelling of braided textile reinforced composites is presented. A macro-scale model considering composite fracture and delamination was suggested to study the composite's response under impact loading conditions. The samples were tested at three energy levels, ranging from 3 J (invisible damage) to 9 J (close to perforation). The dynamic response was studied employing load- and energy-time curves. The damaged samples were characterized with X-ray micro computed-topography. The experimental data were compared to the results of numerical ions; the failure mechanisms under impact loading were identified and analysed. The present work offer modelling capability for analysis of low-velocity impacts with the Hashin damage criterion, the quadratic traction criterion for damage initiation and the Benzeggagh-Kenane criterion for its evolution.

2. Experimental Studies

2.1. Composite Preparation

The braided preform consisted of carbon fibre tows (AKSAca A-42-12k); the matrix material was Bakelite® EPR-L20 epoxy resin that was mixed with EPH-960 hardener at a weight ratio of 100:35, and the mixture was then degassed for approximately 30 minutes. The epoxy resin was injected in to the preform employing a vacuum-assisted resin-infusion method before curing for 24 hours at room temperature followed by 15 hours at 60 °C. The braiding angle in the laminates was 25º and a fibre volume fraction was about 55%. The plates were cut into pieces with dimensions of 55 mm × 55mm × 1.6 mm.

2.2. Drop-weight Test and Characterization

The drop-weight test programme was carried out with a 9250HV Instron Dynatup test system, as shown in Fig. 1. A spike-shape impactor was chosen considering real-life conditions of sports impact collision. The impactor had a flat bottom with a 10 mm diameter and a weight of 6.1646 kg. The testing machine was equiped with an anti-rebound system to prevent multiple impacts on the tested specimen. The low-velocity impact tests were carried out according to ASTM Standard D 7136, with different impact energies (3 J, 6 J and 9 J); this was achieved by varying the initial height of the impactor with a constant mass. The specimens were supported on a pneumatically clamped ring with a 40 mm internal diameter. Magnitudes of time (in ms), energy (in J), force (in kN), deflection (in mm), and velocity (in m/s) were recorded automatically by the system. X-ray micro-tomography (Micro-CT) measurements were performed using an XT H 225 X-ray and CT inspection system supplied by Nikon Metrology Instruments. Samples were scanned using the following settings: 60 kV peak, 150 µA and 2 frames per projection.

Excerpt from ISBN 978-3-00-053387-7

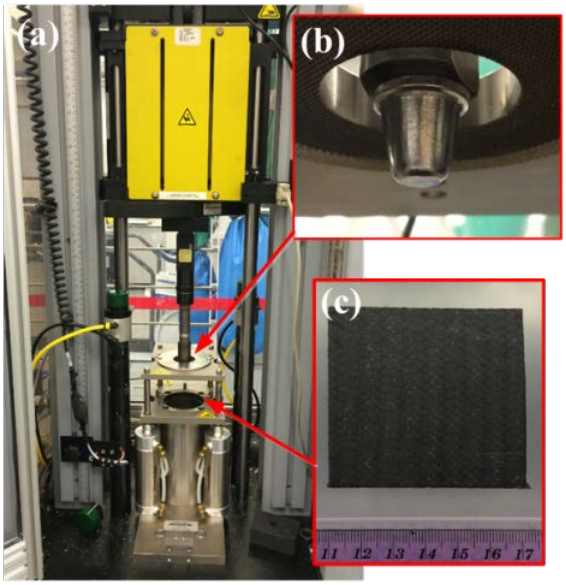

Figure 1 Drop-weight impact test setup (a) with spike-shape impactor (b) and plate of braided composite specimen (c).

3. Finite-element Modelling

3.1. Damage Criteria and Damage Evolution

The Hashin's damage criteria [10] were used to model the damage initiated within the composite. The criteria are described in the following form:

Fibre failure in tension: (σ_{11}>0)
$$\left(\frac{\sigma_{11}}{X_T}\right)^2 + \alpha\frac{\tau_{12}^2}{(S_L)^2} = 1, \quad (1)$$

Fibre failure in compression: (σ_{11}<0)
$$\left(\frac{\sigma_{11}}{X_c}\right)^2 = 1, \quad (2)$$

Matrix failure in tension: (σ_{22}>0)
$$\left(\frac{\sigma_{22}}{Y_T}\right)^2 + \frac{\tau_{12}^2}{(S_L)^2} = 1, \quad (3)$$

Matrix failure in compression: (σ_{22}<0)
$$\left[\left(\frac{Y_C}{2S_T}\right)^2 - 1\right]\frac{\sigma_{22}}{Y_C} + \left(\frac{\sigma_{22}}{2S_T}\right)^2 + \frac{\tau_{12}^2}{(S_L)^2} = 1, \quad (4)$$

where X_T and X_C are the longitudinal (fibre direction) tensile and compressive strength, Y_T and Y_C are the transverse tensile and compressive strengths, S_L and S_T are the longitudinal and transverse shear strength, σ_{ii} (i=1 and 2) and τ_{12} are the effective normal stress components and shear stress component, respectively, and α is a coefficient that determines the contribution of shear stress to fibre tensile initiation criterion.

After damage initiation, the response of the material was computed from

$$\sigma = C_d\varepsilon,$$

where ε is the strain tensor and C_d is the stiffness matrix, which accounts for damage:

Excerpt from ISBN 978-3-00-053387-7

$$C_d = \frac{1}{D}\begin{bmatrix} (1-d_f)E_1 & (1-d_f)(1-d_m)\nu_{21}E_1 & 0 \\ (1-d_f)(1-d_m)\nu_{12}E_2 & (1-d_m)E_2 & 0 \\ 0 & 0 & (1-d_s)GD \end{bmatrix},$$

where

$$D = 1-(1-d_f)(1-d_m)\upsilon_{12}\upsilon_{21},$$

the damage variables d_f, d_m and d_s reflect the current state of fibre damage, matrix damage and shear damage, respectively. E_1, E_2 and G are the longitudinal Young's modulus, the transverse modulus and the shear modulus, respectively. The Poisson ratios are denoted by ν_{12} and ν_{21}. The damage variables (d_f, d_m and d_s) evolve according to the linear damage evolution law based on stress-displacement behaviours in the four failure modes.

3.2. Delamination

Cohesive-zone models were used to simulate the process of delamination between composite layers. The traction stress and separation displacement of the nodes on the surfaces were governed by the traction-separation law, as shown in Eq. 5. According to the law, the area under the curve represents fracture toughness (the critical energy release rate) in a specific fracture mode [12]. The crack was initiated when the following equation was satisfied.

$$\left(\frac{\langle t_n \rangle}{N}\right)^2 + \left(\frac{t_s}{S}\right)^2 + \left(\frac{t_t}{T}\right)^2 = 1, \tag{5}$$

where t_n, t_s and t_t are the traction along the normal (n) and shear (s, t) directions. N, S and T are the respective normal and shear strengths. Damage evolution was defined based on fracture energy; the linear softening behaviour was utilised. The dependency of fracture energy on mixed fracture modes was expressed by the widely used Benzeggagh-Kenane formulation [19], which has the following an analytical form:

$$G^C = G_n^C + (G_s^C - G_n^C)\left\{\frac{G_s^C + G_t^C}{G_n^C + G_s^C + G_t^C}\right\}^\eta, \tag{6}$$

where G_n, G_s and G_t are the works done by tractions and their conjugate relative displacements corresponding to modes I, II and III, respectively. The power, η, is a material parameter, selected as 1.45 for a carbon fibre composite [20].

3.3. Impact Model of Braided Composites

The studied braided composite was modelled with a developed multi-scale modelling approach. In this approach, information was passed across length scales. A unit cell was employed at the meso-scale to describe the braided architecture of the fibre bundles in a previous study and to provide material parameters for the macro-scale model (see details in [21, 22]). The obtained engineering constants and material properties of composites are shown in Tables 1 and 2. Here, the braided composite plate was modelled as a homogeneous material in a macroscopic sense. Continuum shell elements were then used to model the circular specimen plates as shown in Figure 2.

The geometry chosen simulated the circular pneumatic clamp used in the testing machine. The nodes at the model's periphery were fixed in all directions to mimic the experimental process, where the composite plate was pneumatically clamped. The dimensions of the model were the same as the employed experimental setup. Cohesive elements with thickness of 0.01 mm were applied between two plies of the composite. The elastic properties of the cohesive elements are defined as shown in Table 3. The spike-shaped impactor was modelled as a rigid body with a lumped mass equal to the mass used in

Excerpt from ISBN 978-3-00-053387-7

the experimental programme. A level of initial velocity in the vertical direction was prescribed for the impactor, resulting in the corresponding impact energy.

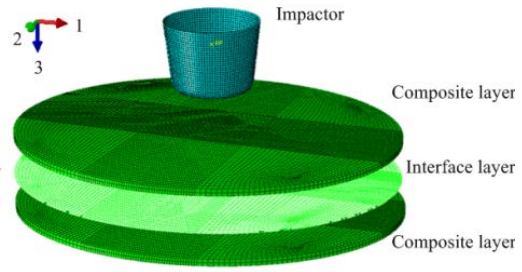

Figure 2 Drop-weight impact FE model with spike-shape impactor: from meso-scale model to macro-scale model.

Table 1. Material properties of carbon A-42 fibre tow [21].

E_1 (GPa)	$E_2=E_3$ (GPa)	$\nu_{12}=\nu_{13}$	ν_{23}	$G_{12}=G_{13}$ (GPa)	G_{23} (GPa)	E_m (GPa)	ν_m
193.93	10.9	0.18	0.35	4.59	3.65	3.3	0.35

Table 2. Material properties of braided composite [22].

E_1 (GPa)	E_2 (GPa)	E_3 (GPa)	ν_{12}	ν_{13}	ν_{23}	G_{12} (GPa)	G_{13} (GPa)	G_{23} (GPa)
36.37	7.4	7.07	1.19	0.026	0.29	16.31	2.72	2.31
X_t (MPa)	X_c (MPa)	Y_t (MPa)	Y_c (MPa)	S_{12} (MPa)	S_{23} (MPa)	G_{ft} (kJ/m^2)	G_{fc} (kJ/m^2)	$G_{mt}=G_{mc}$ (kJ/m^2)
591.57	350	220	200	200	200	81.5	106.3	1

Table 3. Interface properties of braided composite [16, 23].

K_n (GPa/mm)	$K_s=K_t$ (GPa/mm)	T_n (MPa)	$T_s=T_t$ (MPa)	G_n (J/m^2)	$G_s=G_t$ (J/m^2)	η
2.89	2	62.3	92.3	280	790	1.45

4. Results and Discussion

4.1. Impact-load Response of Braided Composites

The drop-weight impact responses of composite are mainly characterised in terms of maximum impact force, energy to peak force and final energy absorption. The load-time curves of the braided composite under impact loading are shown in Fig. 3. Comparing the impact force-time curves for three levels of impact energy, it can be observed that the time to peak force became smaller with an increase of impact velocity. As expected, the peak force increased with an increase in impact energy. However, when the impact energy was 9 J, the peak force was similar to that for the 6 J impact, with a sudden drop. The FE results for the peak force were slightly lower than those in the experimental tests. In summary, the trend of FEM results agreed well with the experimental data.

Energy-absorption behaviours for the braided composite under different impact energies are shown in Fig. 4. The total strain energy and final absorbed energy increased with increasing impact velocity, as

Excerpt from ISBN 978-3-00-053387-7

well as the rate of energy absorption. Furthermore, the FE simulation results can predict the total strain energy.

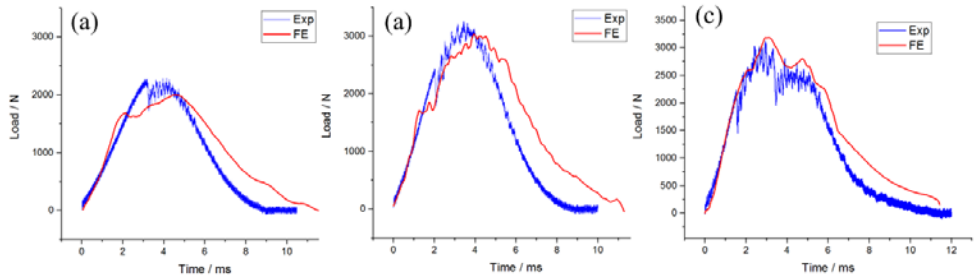

Figure 3 Load-time response of braided composite plate under various impact energies: (a) 3 J; (b) 6 J; (c) 9 J

However, there are noticeable variations when predicting the final absorbed energy after the impact. The final absorbed energy is attributed to barely invisible damage inside the composite when the impact energy is below 6 J. However, when the impact energy was 9 J, small plastic deformation was expected to occur in the composite. Due to the difficulty in obtaining accurate values for fracture energy of each damage mode and the assumptions used in the simulations, the final absorbed energy obtained with FE simulations was smaller than that in the experimental results.

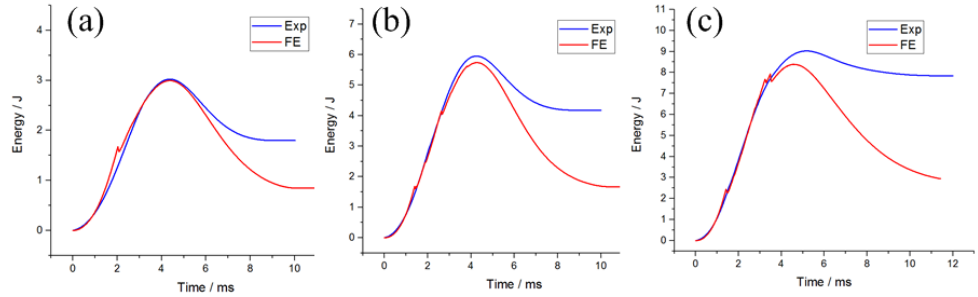

Figure 4 Energy-time response of braided composite plate under various impact energies: (a) 3 J; (b) 6 J; (c) 9 J

4.2. Delamination

Delamination is a common damage mode in layered composite materials. The predicted delamination area at the interface of the braided composite is shown in Fig. 5. It is obvious that the damage area was spread mainly along the fibre direction. With the increasing impact energy, the delamination area grew. The delamination areas obtained from the simulations were compared with the images acquired with CT-scanning. Figure 6 (a) show the front view of the braided composite after the impact; no obvious damage was observed. However, in the cross-section parallel to the surface (Fig. 6(b)), the delamination area (denoted by a darker zone) can be observed. From Fig. 6(c), the crack between two braided plies also indicates the delamination clearly. Compared to Fig. 5 (a), the elliptical shape of delamination area is captured by FE predictions.

5. Conclusions

The response of braided composite to low-velocity impacts was investigated both experimentally and with FE simulations. Impact energy levels ranged from 3 J to 9 J. The present work offer reasonable modelling capabilities for low-velocity impacts. The simulated results were verified by the original experimental data. The results showed that the peak force increased with the increasing impact velocity. The trend of FEM results agreed well with the experimental results. The FE simulation results predicted the total strain energies well, while the calculated levels of the final absorbed energy were smaller than

Excerpt from ISBN 978-3-00-053387-7

those in the experimental tests. The main damage mechanisms of the braided composite under low-velocity impact were delamination and matrix failure modes. The delamination damage area was mainly along the fibre direction and could be accurately predicted with the FE-based approach.

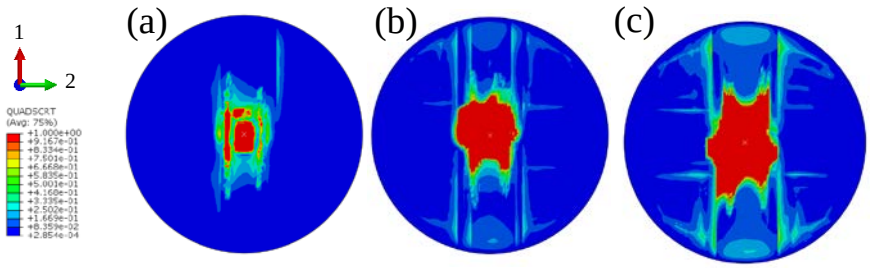

Figure 5 Interface delamination of braided composite plate under various impact energies: (a) 3 J; (b) 6 J; (c) 9 J

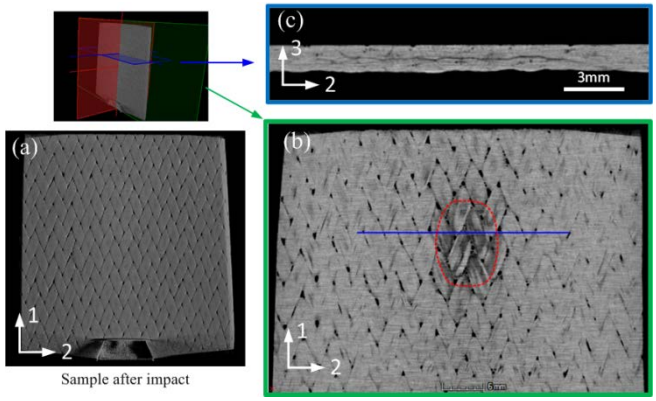

Figure 6 CT scan of morphology of braided composite plate under impact energy of 3 J: (a) whole structure after impact; (b) interface delamination area; (c) delamination in cross-section view

Acknowledgments

CW is grateful for the financial support by NTU through the PhD scholarship award. The authors are grateful for the technical support by the Sports Technology Institute of Loughborough University.

References

[1] S.G. Kulkarni, X.L. Gao, S.E. Horner, J.Q. Zheng and N.V. David. Ballistic helmets- their design, materials, and performance against traumatic brain injury. *Composite Structures*, 101: 313-31, 2013.

[2] Y. Wan, Y. Wang and B. Gu. Finite element prediction of the impact compressive properties of three-dimensional braided composites using multi-scale model. *Composite Structures*, 128: 381-94, 2015.

[3] Y. Tatar, N. Ramazanoglu, A.F. Camliguney, E.K. Saygi and H.B. Cotuk. The effectiveness of shin guards used by football players. *Journal of Sports Science and Medicine*, 13: 120-127, 2014.

[4] C.S. Lopes, O. Seresta, Y. Coquet, Z. Gürdal, P.P. Camanho and B. Thuis. Low-velocity impact damage on dispersed stacking sequence laminates. Part I: Experiments. *Composites Science and Technology*, 69(7): 926-936, 2009.

[5] J.P. Hou, N. Petrinic, C. Ruiz, and S.R. Hallett. Prediction of impact damage in composite plates. *Composites Science and Technology*, 60(2): 273-281, 2000.

[6] M. Alemi-Ardakani, A. S. Milani, S. Yannacopoulos, and H. Borazghi. A rapid approach for predication and discrete lay-up optimization of glass fiber/polypropylene composite laminates

Excerpt from ISBN 978-3-00-053387-7

under impact. *International Journal of Impact Engineering*, 84: 134–144, 2015.

[7] C.S. Lopes, P.P. Camanho, Z. Gürdal, P. Maimí, and E.V. González. Low-velocity impact damage on dispersed stacking sequence laminates. Part II: Numerical simulations. *Composites Science and Technology*, 69(7): 937-947, 2009.

[8] M. Moura and A. Marques, Prediction of low velocity impact damage in carbon-epoxy laminates. *Composites: Part A*, 33: 361-368, 2002.

[9] S.W. Tsai and E.M. Wu. A general theory of strength for anisotropic materials. *Journal of Composite Materials*, 5(1): 58-80, 1971.

[10] Z. Hashin. Fatigue failure criteria for unidirectional fiber composites. *Journal of Applied Mechanics*, 48(4): 846, 1981.

[11] V. Tita, J. de Carvalho and D. Vandepitte. Failure analysis of low velocity impact on thin composite laminates: experimental and numerical approaches. *Composite Structures*, 83: 413–428, 2008.

[12] D. Feng and F. Aymerich. Finite element modelling of damage induced by low-velocity impact on composite laminates. *Composite Structures*, 108: 161–171, 2014.

[13] E.H. Kim, M.S. Rim, I. Lee, T.K. Hwang. Composite damage model based on continuum damage mechanics and low velocity impact analysis of composite plates. *Composite Structures*, 95: 123-134, 2013.

[14] M.V. Donadon, L. Iannucci, B.G. Falzon, J.M. Hodgkinson, S.F.M. de Almeida. A progressive failure model for composite laminates subjected to low velocity impact damage. *Composite Structures*, 86 (11–12):1232–1252, 2008.

[15] S. Long, X. Yao and X. Zhang. Delamination prediction in composite laminates under low-velocity impact. *Composite Structures*, 132: 290-298, 2015.

[16] A. Qiu, K. Fu, W. Lin, C. Zhao and Y. Tang. Modelling low-speed drop-weight impact on composite laminates. *Materials and Design*, 60: 520–531, 2014.

[17] R.K. Gideon, F. Zhang, L. Wu, B. Sun and B. Gu. Damage behaviors of woven basalt-unsaturated polyester laminates under low-velocity impact. *Journal of Composite Materials*, 49(17): 2103–2118, 2015.

[18] W. Wang, X. Wan, J. Zhou, M. Zhao, Y. Li, S. Shang and X Gao. Damage and Failure of a Laminated Carbon Fiber Reinforced Composite under Low Velocity Impact. *Journal of Aerospace Engineering*, 27(2): 308–317, 2014.

[19] M.L. Benzeggagh and M. Kenane. Measurement of mixed-mode delamination fracture toughness of unidirectional glass/epoxy composites with mixed-mode bending apparatus, *Composite Science and Technology*, 56: 439-449, 1996.

[20] P.P. Camanho, C.G. Davila and M.F. de Moura. Numerical simulation of mixed-mode progressive delamination in composite materials, *Journal of Composite. Material*, 37 (16): 1415-1438, 2003.

[21] X. Ji, C. Wang, B.P. Francis, E.S.M. Chia, L. Zheng, J. Yang and Z. Chen. Mechanical and interfacial properties characterisation of single carbon fibres for composite applications. *Experimental Mechanics*, 1057–1065, 2015.

[22] C. Wang, Y. C. Zhong, P. F. B. Adaikalaraj, X. B. Ji, A. Roy, V. V. Silberschmidt and Z. Chen. Strength prediction for bi-axial braided composites by a multi-scale modelling approach, *Journal of Materials Science*, 51: 6002-6018, 2016.

[23] A. Faggiani and B.G. Falzon. Predicting low-velocity impact damage on a stiffened composite panel, *Composites Part A: Applied Science and Manufacturing*, 41(6): 737-749, 2010.

Excerpt from ISBN 978-3-00-053387-7